Supporting Information

Solution-processed ZnO/SnO_2 bilayer ultraviolet phototransistor with high responsivity and fast photoresponse

Hojoong Choi,[a] Sehun Seo,[a] Jong-Hoon Lee,[a] Sang-Hyun Hong,[b] Jaesun Song,[a] Seungkyu Kim,[a] Sang-Youp Yim,[b] Kwanghee Lee,[a] Seong-Ju Park,[a] and Sanghan Lee*[a]

[a] School of Materials Science and Engineering, Gwangju Institute of Science and Technology, Gwangju, 61005, Republic of Korea

[b] Advanced Photonics Research Institute, Gwangju Institute of Science and Technology, Gwangju 61005, Republic of Korea

*E-mail address: sanghan@gist.ac.kr

Characteristics of solution-processed SnO_2 thin film and ZnO nanoparticles

The thickness of the SnO_2 thin films inserted using 0.1, 0.15 and 0.2 M SnO_2 precursor solutions were determined by the field emission scanning electron microscopy (FESEM) cross-sectional images to be approximately 12.84, 15.32 and 19.36 nm, respectively, as shown in Fig. S1a–c. It was found that the thickness of SnO_2 thin films dependent on the precursor concentration of SnO_2.

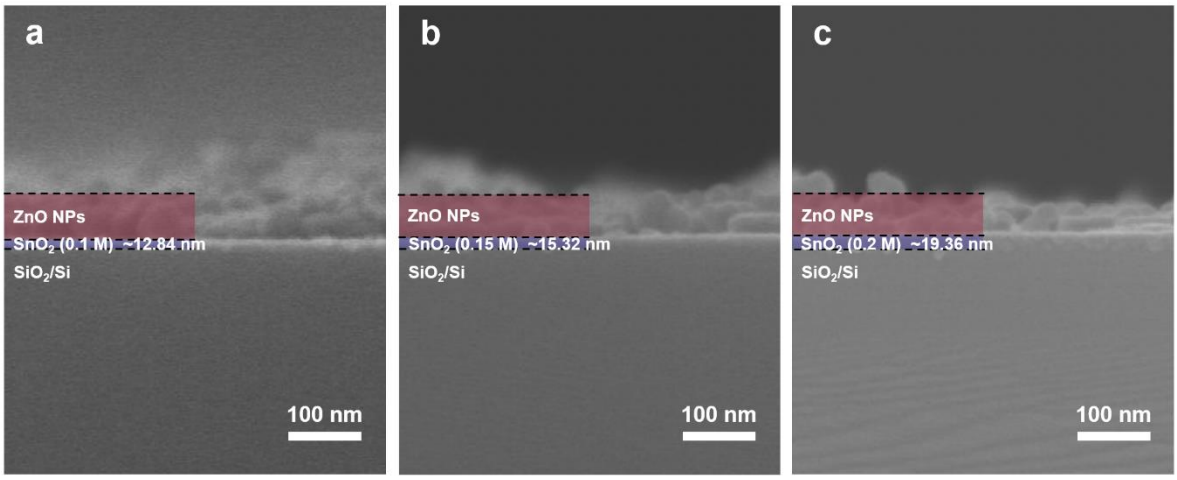

Fig. S1 Field emission scanning electron microscopy (FESEM) cross-sectional images of ZnO NPs/SnO_2 bilayer film with SnO_2 thin films inserted using (a) 0.1, (b) 0.15, and (c) 0.2 M SnO_2 precursor solutions.

Electrical characteristics of ZnO single-layer and ZnO/SnO_2 bilayer UV phototransistors

The field effect mobility (μ_{FE}), on/off current ratio, subthreshold swing and threshold voltage of ZnO single-layer and ZnO/SnO_2 bilayer UV phototransistors with SnO_2 carrier transport layer inserted using 0.1, 0.15, and 0.2 M SnO_2 precursor solutions were summarized as shown in Table S1. The parameters were obtained from the transfer characteristics shown in Fig. 2a–d.

Table S1 Electrical characteristics of ZnO single-layer and ZnO/SnO_2 bilayer UV phototransistors and their dependence on thickness determined by the precursor concentration of inserted SnO_2 carrier transport layer.

Active layer	Thickness of inserted SnO_2 carrier transport layer (nm)	Field effect mobility ($cm^2\ V^{-1}\ s^{-1}$)	On/off current ratio	Subthreshold swing ($V\ dec^{-1}$)	Threshold voltage (V)
ZnO single-layer	0	2.61×10^{-4}	~10^3	1.26	17.5
ZnO/SnO_2 (0.1 M) bilayer	12.84	3.66	~10^8	0.56	3.36
ZnO/SnO_2 (0.15 M) bilayer	15.32	6.05	~10^8	0.34	2.65
ZnO/SnO_2 (0.2 M) bilayer	19.36	8.51	~10^7	0.42	1.13

Field effect mobility of the SnO_2 carrier transport layers

The representative transfer characteristics of the SnO_2 layers fabricated with 0.1, 0.15, and 0.2 M SnO_2 precursor solutions were measured at drain voltage (V_{DS}) of 5 V under ambient dark condition as shown in Fig. S2a. The μ_{FE} of the SnO_2 layers was found to be dependent on its thickness, which is determined by the SnO_2 concentration in the solution used to deposit the SnO_2 thin film as shown in Fig. S2b.

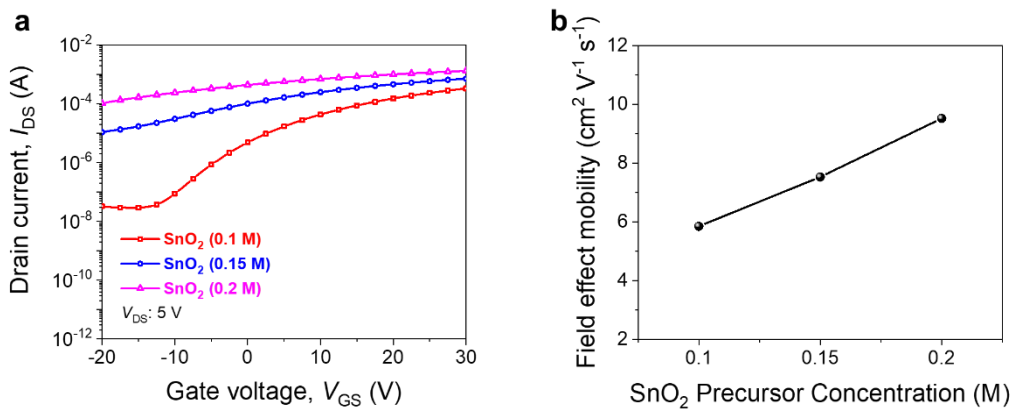

Fig. S2 (a) Transfer characteristics of the SnO_2 layer fabricated with 0.1, 0.15 and, 0.2 M SnO_2 precursor solutions measured at V_{DS} of 5 V under ambient dark condition and (b) field effect mobility of the SnO_2 layer as a function of the SnO_2 precursor concentration.

UV intensity dependent responsivity of ZnO single-layer and ZnO/SnO_2 bilayer UV photo-transistors

The responsivity of the ZnO single-layer and ZnO/SnO_2 bilayer UV phototransistors with SnO_2 carrier transport layer inserted using 0.1, 0.15 and, 0.2 M SnO_2 precursor solutions as a function of UV intensity in the range from 0.53 to 1.35 mW cm^{-2} were shown in Fig. S3. The parameters were obtained from the I_{DS}–V_{DS} characteristics shown in Fig. 3a–d at V_{DS} of 5 V. All the ZnO/SnO_2 bilayer UV phototransistors regardless of precursor concentration of inserted SnO_2 layer exhibited higher UV photoresponse characteristics than those of ZnO single-layer UV phototransistor in all range of UV intensities as shown in Fig. S3.

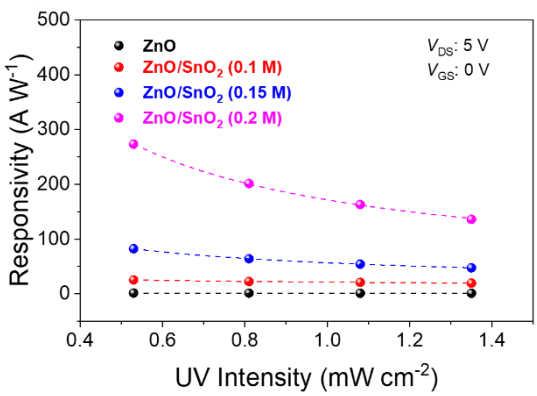

Fig. S3 Responsivity of ZnO single-layer and ZnO/SnO_2 bilayer UV phototransistors with SnO_2 carrier transport layer inserted using 0.1, 0.15 and, 0.2 M SnO_2 precursor solutions at a V_{DS} of 5 V and V_{GS} of 0 V as a function of UV intensity in the range from 0.53 to 1.35 mW cm^{-2}.

Modulation of the responsivity and detectivity of ZnO/SnO_2 bilayer UV phototransistor by controlling gate voltage (V_{GS})

The responsivity tended to increase with increasing V_{GS}, whereas the detectivity tended to increase with decreasing V_{GS} up to −1 V and then decreased with a decrease in V_{GS} below –1 V as shown in Fig S4. We attribute this behavior to the fact that the responsivity is predominantly modulated by the photocurrent, whereas the detectivity is predominantly modulated by the dark current.[1]

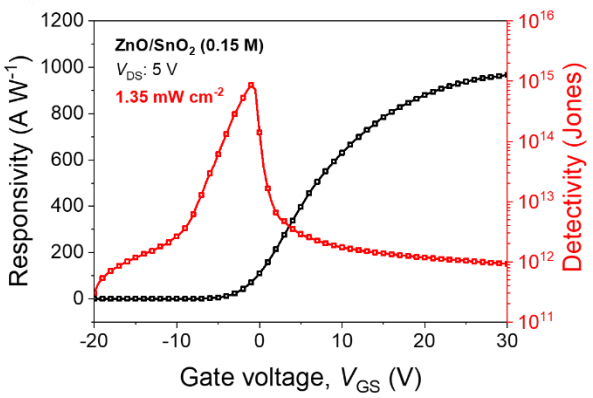

Fig. S4 Responsivity and detectivity of ZnO/SnO_2 (0.15 M) bilayer UV phototransistor as a function of V_{GS} at a V_{DS} of 5 V under 1.35 mW cm^{-2} UV illumination.

UV photoresponse characteristics of ZnO NRs and ZnO NRs/SnO_2 UV photodetectors

The length of ZnO nanorods (NRs) grown at 90 ℃ for 2 h using the ZnO single-layer and ZnO/SnO_2 (0.15 M) bilayer UV phototransistors as the seed layer was estimated to be approximately 450~500 nm by FESEM cross-sectional images as shown in Fig. S5a and b. It was found that the grown ZnO NRs using ZnO single-layer and ZnO/SnO_2 bilayer UV phototransistors as the seed layer demonstrated almost the same length, density and aspect ratio of ZnO NRs as shown in Fig. S5a–d.

The photocurrent in the I_{DS}–V_{DS} characteristics of the ZnO NRs and ZnO NRs/SnO_2 UV photodetectors with optimized SnO_2 carrier transport layer inserted using 0.15 M SnO_2 precursor solution was shown in Fig. S6a and b, respectively. The ZnO NRs/SnO_2 UV photodetector exhibited the higher photocurrent than the photocurrent of ZnO NRs photodetector as shown in Fig. S5a and b. In the time-dependent photoresponse of the ZnO NRs and ZnO NRs/SnO_2 UV photodetector, respectively shown in Fig. S6c and d, the ZnO NRs/SnO_2 UV photodetector exhibited higher photocurrent and resulting high responsivity.[2] Furthermore, from the normalized time-dependent photoresponse of ZnO NRs and ZnO NRs/SnO_2 UV photodetector under 1.35 mW cm^{-1} UV illumination in Fig. S6e and f, estimated response and recovery time of ZnO NRs UV photodetector were 13.8 and 7.16 s, respectively and the ZnO NRs/SnO_2 UV photodetector exhibited faster UV photoresponse which were estimated as 11.6 and 4.47 s, respectively. These results were attributed to efficient extraction of photogenerated electrons from the ZnO UV sensitive layer through the SnO_2 carrier transport layer with high μ_{FE} was also applied to the case of ZnO NRs UV sensitive layer.[3]

From the I_{DS}–V_{DS} characteristics shown in Fig. 6Sa and b at V_{DS} of 5 V, the responsivity of ZnO NRs and ZnO NRs/SnO_2 UV photodetectors as a function of UV intensity in the range from 0.53

to 1.35 mW cm^{-1} were obtained as shown in Fig. S7. As shown in Fig. S7, the responsivity of ZnO NRs/SnO_2 UV photodetector (3251.69 A W^{-1}) was improved by 1.6 times than that of ZnO NRs UV photodetector (2023.67 A W^{-1}) under 0.53 mW cm^{-2} and 365 nm wavelength UV illumination.

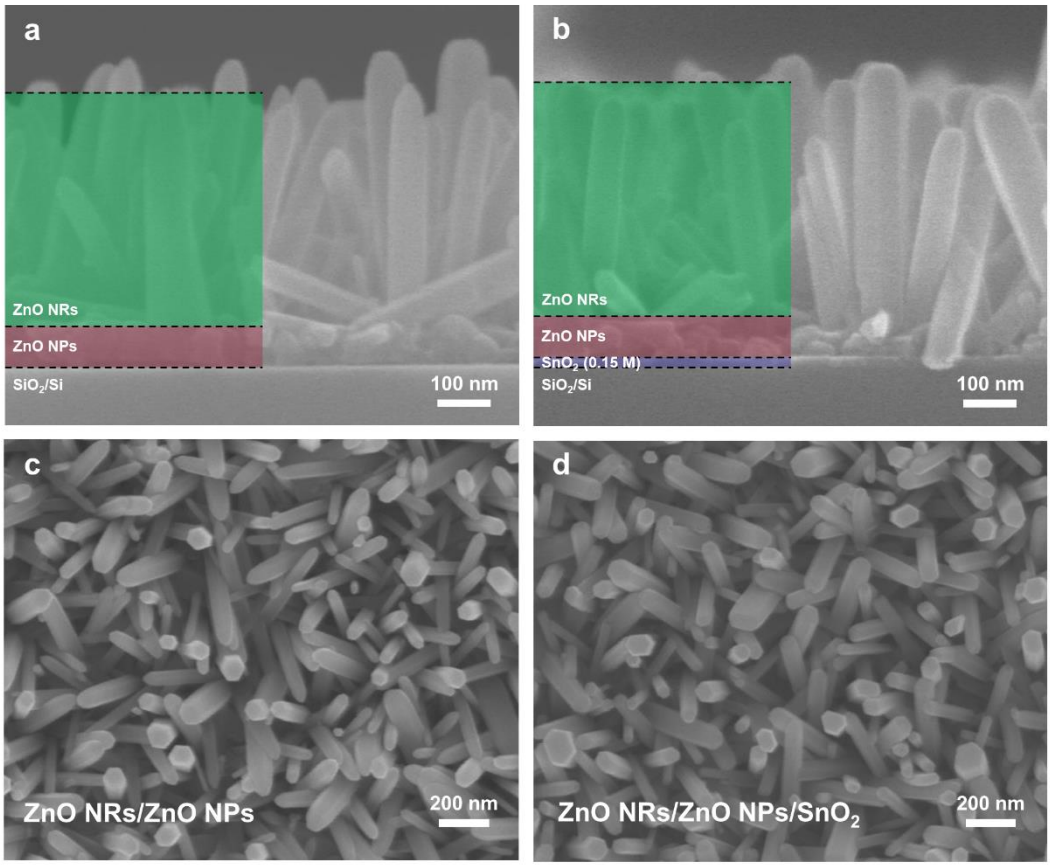

Fig. S5 FESEM images of the grown ZnO NRs using (a, c) ZnO single-layer and (b, d) ZnO/SnO_2 bilayer UV phototransistors as the seed layer.

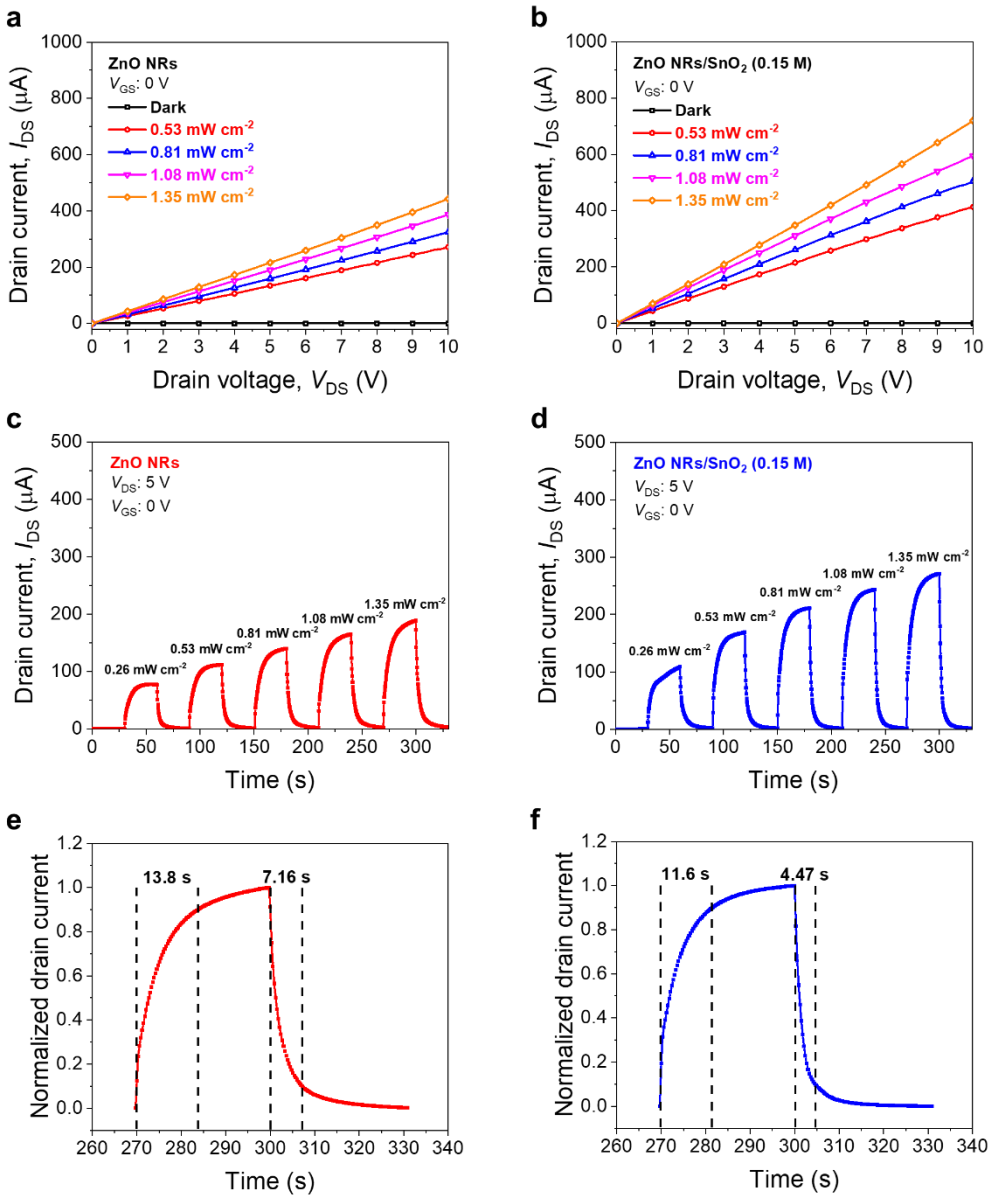

Fig. S6. I_{DS}–V_{DS} characteristics of the (a) ZnO NRs and (b) ZnO NRs/SnO_2 (0.15 M) UV photodetectors under dark and the range from 0.53 to 1.35 mW cm^{-2} UV illumination. Time-dependent UV photoresponse of (c) ZnO NRs and (d) ZnO NRs/SnO_2 (0.15 M) UV photodetectors at a V_{DS} of 5 V and V_{GS} of 0 V. Normalized time-dependent UV photoresponse of (e) ZnO NRs and (f) ZnO NRs/SnO_2 (0.15 M) UV photodetectors under 1.35 mW cm^{-2} UV illumination.

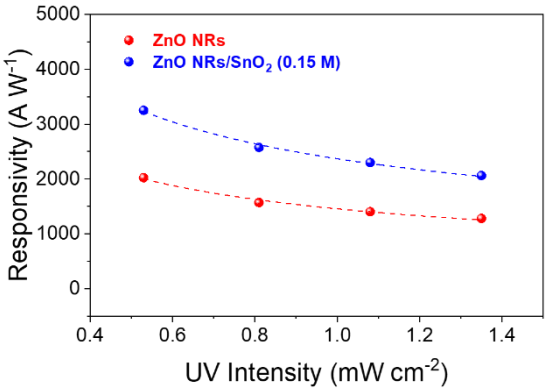

Fig. S7 Responsivity of ZnO NRs and ZnO NRs/SnO_2 (0.15 M) UV photodetectors at a V_{DS} of 5 V and V_{GS} of 0 V as a function of UV intensities in the range from 0.53 to 1.35 mW cm^{-2}.

Comparison of UV photoresponse characteristics of the ZnO/SnO_2 bilayer UV phototransistor with various ZnO-based heterojunction UV sensing devices

As shown in Table S2, the UV photoresponse characteristics including responsivity, detectivity and photoresponse time of ZnO/SnO_2 bilayer UV phototransistor and ZnO NRs/SnO_2 UV photodetector in this study were greater than other ZnO-based heterojunction UV sensing devices including UV phototransistor and photodetector. Although the responsivity of some ZnO-based heterojunction UV sensing devices with graphene or MoS_2 inserted exhibited higher values of responsivity, our ZnO/SnO_2 bilayer UV phototransistor exhibited high detectivity and fast photoresponse than other ZnO-based heterojunction UV photodetectors. Considering the fact that no complex transfer process of graphene or MoS_2 is required for device fabrication of our ZnO/SnO_2 bilayer UV phototransistor, it has a great deal of potential for high-performances, low-cost and large-area solution-processed UV phototransistor. In addition, the ZnO NRs/SnO_2 UV photodetector exhibited even high detectivity and fast photoresponse and simultaneously exhibited comparable value of responsivity with the graphene or MoS_2 inserted UV sensing devices.

Table S2 Comparison of responsivity, detectivity and photoresponse time with various ZnO-based heterojunction UV sensing devices.

Active layer	Wavelength of UV light source (nm)	Responsivity (A W^{-1})	Detectivity (Jones)	Photoresponse time (s)	References
ZnO NRs/graphene	365	3×10^5 (at V_{DS} = 1 V)	-		(3)
ZnO QD/graphene/SAM	335	~2.4×10^7 (at V_{GS} = 5.6 V)	5.1×10^{13}	2.3 (recovery)	(4)
Au/$CdMoO_4$/ZnO	350	0.321 (at 5 V)	-	16 (response) 9 (recovery)	(5)
Ag NPs/ZnO	380	2.86	-	~15 (response)	(6)

		(at 5 V)		~330 (recovery)	
ZnO/Ag NW/ZnO	365	2.4 (at 1 V)	6.8×10^{12} (at 1 V)	3.53 (response) 3.67 (recovery)	(7)
ZnO NWs/graphene foam	365	~7 (at 5 V)	-	9.5 (response) 38 (recovery)	(8)
ZnO NFs/graphene	350	350 (at 1 V)	-	10 (response) 67 (recovery)	(9)
ZnO QD/h-BN/graphene/GaN	245	1.92×10^{3}	1.02×10^{13}	6 (response) 3 (recovery)	(10)
ZnO QD/MoS_2	220	2.27×10^{3} (at V_{DS} = 1 V, V_{GS} = 30 V)	$1.6 \sim 2.2 \times 10^{11}$ (V_{GS} = 0 ~ 30 V)	24.64 (response) 3.68 (recovery)	(11)
ZnO/SnO_2 bilayer	365	82.28 (at V_{DS}= 5 V, V_{GS} = 0 V)	7.79×10^{13} (at V_{DS}= 5 V, V_{GS} = 0 V)	2.07 (response) 1.59 (recovery)	This work
ZnO NRs/SnO_2	365	3.25×10^{3} (at V_{DS}= 5 V, V_{GS} = 0 V)	2.11×10^{14} (at V_{DS}= 5 V, V_{GS} = 0 V)	11.6 (response) 4.47 (recovery)	This work

References

1 D. Kufer, T. Lasanta, M. Bernechea, F. H. Koppens and G. Konstantatos, *ACS Photonics*, 2016, **3**, 1324–1330.

2 S. Jeong, M. W. Kim, Y.-R. Jo, Y.-C. Leem, W.-K. Hong, B.-J. Kim and S.-J. Park, *Nano Energy*, 2016, **30**, 208–216.

3 V. Q. Dang, T. Q. Trung, D. I. Kim, L. T. Duy, B. U. Hwang, D. W. Lee, B. Y. Kim, L. D. Toan and N. E. Lee, *Small*, 2015, **11**, 3054–3065.

4 D. Shao, J. Gao, P. Chow, H. Sun, G. Xin, P. Sharma, J. Lian, N. A. Koratkar and S. Sawyer, *Nano Lett.*, 2015, **15**, 3787–3792.

5 W. Ouyang, F. Teng, M. Jiang and X. Fang, *Small*, 2017, **13**, 1702177.

6 X. Wang, K. Liu, X. Chen, B. Li, M. Jiang, Z. Zhang, H. Zhao and D. Shen, *ACS Appl. Mater. Interfaces*, 2017, **9**, 5574–5579.

7 Z. Yang, M. Wang, X. Song, G. Yan, Y. Ding and J. Bai, *J. Mater. Chem. C*, 2014, **2**, 4312–4319.

8 B. D. Boruah, A. Mukherjee, S. Sridhar and A. Misra, *ACS Appl. Mater. Interfaces*, 2015, **7**, 10606–10611.

9 Y. B. Lee, S. K. Kim, Y. R. Lim, I. S. Jeon, W. Song, S. Myung, S. S. Lee, J. Lim and K.-S. An, *ACS Appl. Mater. Interfaces*, 2017, **9**, 15031–15037.

10 Y. Lu, Z. Wu, W. Xu and S. Lin, *Nanotechnology*, 2016, **27**, 48LT03.

11 G. Nazir, M. F. Khan, I. Akhtar, K. Akbar, P. Gautam, H. Noh, Y. Seo, S.-H. Chun and J. Eom, *RSC Adv.*, 2017, **7**, 16890–16900.